El Niño–Southern Oscillation sensitivity to cumulus entrainment in a coupled general circulation model

Daehyun Kim,[1] Yeon-Soo Jang,[2] Dong-Hoon Kim,[3] Young-Ho Kim,[2] Masahiro Watanabe,[4] Fei-Fei Jin,[5] and Jong-Seong Kug[2]

Received 6 July 2011; revised 26 August 2011; accepted 14 September 2011; published 22 November 2011.

[1] A series of 200 year long integrations is performed using the Geophysical Fluid Dynamics Laboratory CM2.1 by varying the Tokioka parameter, a minimum entrainment rate threshold in the cumulus parameterization. Changing the threshold alters both the tropical Pacific mean state and the El Niño–Southern Oscillation (ENSO) variability. Increasing the Tokioka parameter causes a basin-wide cooling in the tropical Pacific with the reduction of high clouds. The degree of cooling in the western part of the basin is bigger than that in the east. As a result, the east–west asymmetry in the tropical Pacific sea surface temperature (SST) decreases with increasing the Tokioka parameter. Accompanied with the reduced east–west SST asymmetry are the increase of mean precipitation over the eastern Pacific and the eastward shift of the atmospheric responses to the ENSO-related SST forcing. The eastward shifted wind stress anomaly associated with ENSO leads to the stronger ENSO variability. In this way the magnitude of ENSO simulated in this model increases with the Tokioka parameter. Implication of our results on the relationship between the tropical Pacific mean state and ENSO is discussed.

Citation: Kim, D., Y.-S. Jang, D.-H. Kim, Y.-H. Kim, M. Watanabe, F.-F. Jin, and J.-S. Kug (2011), El Niño–Southern Oscillation sensitivity to cumulus entrainment in a coupled general circulation model, *J. Geophys. Res.*, *116*, D22112, doi:10.1029/2011JD016526.

1. Introduction

[2] It has long been challenging to simulate the amplitude of El Niño–Southern Oscillation (ENSO) correctly in state-of-the-art climate models. The wide range of ENSO amplitudes simulated in the coupled ocean-atmosphere general circulation models (CGCMs) inhibits a reliable prediction of the characteristics of ENSO in a changing climate [*Guilyardi et al.*, 2009a]. A number of studies have met the challenge of understanding the mechanism by which the amplitude of ENSO is controlled in the CGCMs [*Li and Hogan*, 1999; *Wu et al.*, 2007; *Kim et al.*, 2008; *Neale et al.*, 2008; *Guilyardi et al.*, 2009b; *Ham et al.*, 2010]. They showed that the characteristics of ENSO, including its amplitude, simulated in the CGCMs are sensitive to the coupled mean state [*Li and Hogan*, 1999] and the configurations of the atmospheric component model, especially its cumulus convection parameterization [*Wu et al.*, 2007; *Kim et al.*, 2008; *Neale et al.*, 2008; *Guilyardi et al.*, 2009b]. *Kim et al.* [2008] demonstrated that the amplitude and periodicity of ENSO simulated in the Seoul National University (SNU) CGCM was largely affected by the inclusion of the cumulus momentum transport (CMT). CMT shifts the mean precipitation, mean trade winds, and the ENSO-related westerly anomalies eastward; thereby it enhances the magnitude of ENSO and lengthens the period of ENSO. *Neale et al.* [2008] also showed that the characteristics of the ENSO were significantly affected by the inclusion of CMT and a dilution approximation for the calculation of convective available potential energy using the simulations with the Community Climate System Model version 3 (CCSM3). In their simulations, CMT plays a similar role as in SNU CGCM shown in the work of *Kim et al.* [2008] and the dilution approximation provides enhanced intraseasonal variability. Both changes contribute to the stronger ENSO amplitude and the longer period of ENSO in CCSM3.

[3] Recently, *Watanabe et al.* [2011] showed that the magnitude of ENSO simulated in the model for interdisciplinary research on climate version 5 (MIROC5) is highly sensitive to a parameter in their convection scheme. In their results, about 13% of reduction in the constant that regulates efficiency of the entrainment in the cumulus parameterization results in about 270% of amplification of the ENSO variability. They attributed such a high sensitivity of the ENSO variability in MIROC5 to the east–west movement of the ENSO-related atmospheric responses with varying the parameter. In their simulations, the stronger ENSO variability

[1]Lamont-Doherty Earth Observatory, Columbia University, Palisades, New York, USA.
[2]Korea Ocean Research and Development Institute, Ansan, South Korea.
[3]Department of Atmospheric Science, Yonsei University, Seoul, South Korea.
[4]Atmosphere and Ocean Research Institute, University of Tokyo, Kashiwa, Japan.
[5]Department of Meteorology, University of Hawai'i at Mānoa, Honolulu, Hawaii, USA.

0148-0227/11/2011JD016526

Table 1. Experiments With Changing the Tokioka Parameter in a Coupled GCM[a]

Experiment	Tokioka Parameter (α)	σ_{nino3} (°C)	$\sigma_{nino3.4}$ (°C)	σ_{nino4} (°C)
tok002	0.002	1.14	1.18	0.95
tok008	0.008	1.20	1.22	1.00
tok025	0.025	1.33	1.37	1.20
tok040	0.040	1.46	1.51	1.31

[a]Here σ_{nino3}, $\sigma_{nino3.4}$, and σ_{nino4} denote the standard deviation of the SST anomalies in the Niño 3, Niño 3.4, and Niño 4 regions, respectively.

is exhibited when the ENSO-related atmospheric anomalies are elongated more to the eastern Pacific. Furthermore, they argued that the position of the atmospheric anomalies was related to the degree of dryness in the eastern Pacific.

[4] In this study, we present results from simulations using the Geophysical Fluid Dynamics Laboratory (GFDL) coupled model version 2.1 (CM2.1) with different values of a minimum entrainment rate threshold in the convection scheme. The Tokioka modification [*Tokioka et al.*, 1988] implemented in CM2.1 suppresses convective plumes when entrainment rates calculated in the cumulus parameterization are less than the threshold that varies inversely with the planetary boundary layer (PBL) depth. In this modification, the threshold value is set as $\mu_{min} = \alpha/D$, where D is the PBL depth and α, the Tokioka parameter, is a nonnegative constant. The use of a larger α value enhances mean entrainment rate simulated in the model, by suppressing convective plumes with a small entrainment rate. Because the less entraining, deep plume is the dominant source of water in the upper troposphere, the amount of high clouds is also affected by the minimum entrainment rate threshold. The Tokioka parameter has been shown to have significant impacts on the atmospheric variability simulated in the atmospheric component model of CM2.1. For example, it affects the statistics of simulated tropical cyclone-like vortex in the idealized framework [*Held and Zhao*, 2008], the simulation of the Madden-Julian Oscillation (MJO) [*Lee et al.*, 2008; *Sobel et al.*, 2010], and the sensitivity of the Hadley circulation to the extratropical thermal forcing [*Kang et al.*, 2008].

[5] In short, the atmospheric variability such as tropical cyclone and MJO are largely affected by the Tokioka parameter in this model, and the radiation balance of the model would change with the same parameter. A reasonable expectation based on these facts would be that the Tokioka parameter has a significant impacts on ENSO simulated in this model, because the characteristics of ENSO simulated in CGCMs are largely affected by the atmospheric response to the ENSO-related SST forcing, and the tropical Pacific mean state. The goal of the current study is to understand the sensitivity of simulated ENSO to this parameter.

[6] The paper is organized as follows. We introduce the model used very briefly, and the Tokioka parameter with some details in section 2. The impacts of the Tokioka parameter on the tropical Pacific mean state and the magnitude of ENSO in our experiments are shown in section 3. In section 4, the similarities and differences between our study and that of *Watanabe et al.* [2011] are discussed. Also discussed in section 4 are other ENSO mechanisms that are not responsible for the changes in the ENSO variability in this model. Summary and conclusion of the current work are given in section 5.

2. Model and Experimental Design

[7] The oceanic component of CM2.1 is the Modular Ocean Model version 4.1p1 (MOM4.1p1) [*Griffies et al.*, 2005; *Gnanadesikan et al.*, 2006]. MOM4.1p1 has 1° × 1° horizontal resolution telescoping to 1/3° meridional spacing near the equator, and 50 vertical levels. The atmospheric component of CM2.1 is the GFDL Atmospheric Model version 2p13, (AM2p13) [*Delworth et al.*, 2006], with a 2° (latitude) by 2.5° (longitude) grid spacing and 24 vertical levels. A diffusion-type CMT parameterization is included in AM2p13 [*Delworth et al.*, 2006]. Readers are referred to the reference documentations for detailed descriptions of both component models. Note that CM2.1 has been used for a suite of climate change experiments for the Intergovernmental Panel on Climate Change Fourth Assessment Report [*Knutson et al.*, 2006].

[8] A series of 200 year long simulations is conducted using CM2.1, by varying the Tokioka parameter in the cumulus parameterization. *Wittenberg* [2009] showed that the characteristics of ENSO changed in intercentennial time scale in CM2.1. To prevent any possible sampling issues regarding the representativeness of ENSO simulated in each experiment, we performed each simulation for 200 years. *Stevenson et al.* [2010] showed that more than 200 years is required to obtain robust statistics for the difference between ENSO amplitudes obtained from two independent CGCM simulations. The Tokioka parameter, which determines the overall magnitude of the entrainment for convective plumes, is varied from 0.002 to 0.04 with irregular intervals in between in the simulations performed (Table 1). Hereafter, tok002 represents the experiment in that the value of the Tokioka parameter is 0.002. Likewise, we used 0.008, 0.025, and 0.04 as the Tokioka parameter for tok008, tok025, and tok040 experiments, respectively. The values of the Tokioka parameters used in this study cover enough parameter space so that the smallest one (0.002) is close to the minimum possible value (i.e., zero) and the largest one (0.04) is close to the maximum possible value for the model to retain reasonable global mean temperature. The cold drift in SST, which occurs when the Tokioka parameter larger than 0.04 is used, inhibit a use of wider range of the parameter as in other studies (e.g., 0–0.2 in the work of *Frierson et al.* [2011]) that used an atmosphere-only model, and prescribe SST as a boundary condition. The tok025 $\alpha = 0.025$ is the experiment using the value given in the standard version of CM2.1.

3. Results

[9] The tropical Pacific mean climate and ENSO simulated in the standard version of CM2.1 (tok025 in this study) are documented in great detail in the work of *Wittenberg et al.* [2006]. Here we focus on the sensitivity of these aspects of the tropical Pacific climate to the Tokioka parameter and refer to *Wittenberg et al.* [2006] for detailed features of tropical mean climate and ENSO in this model.

[10] To demonstrate the sensitivity of ENSO amplitude to the Tokioka parameter, Figure 1 shows the standard

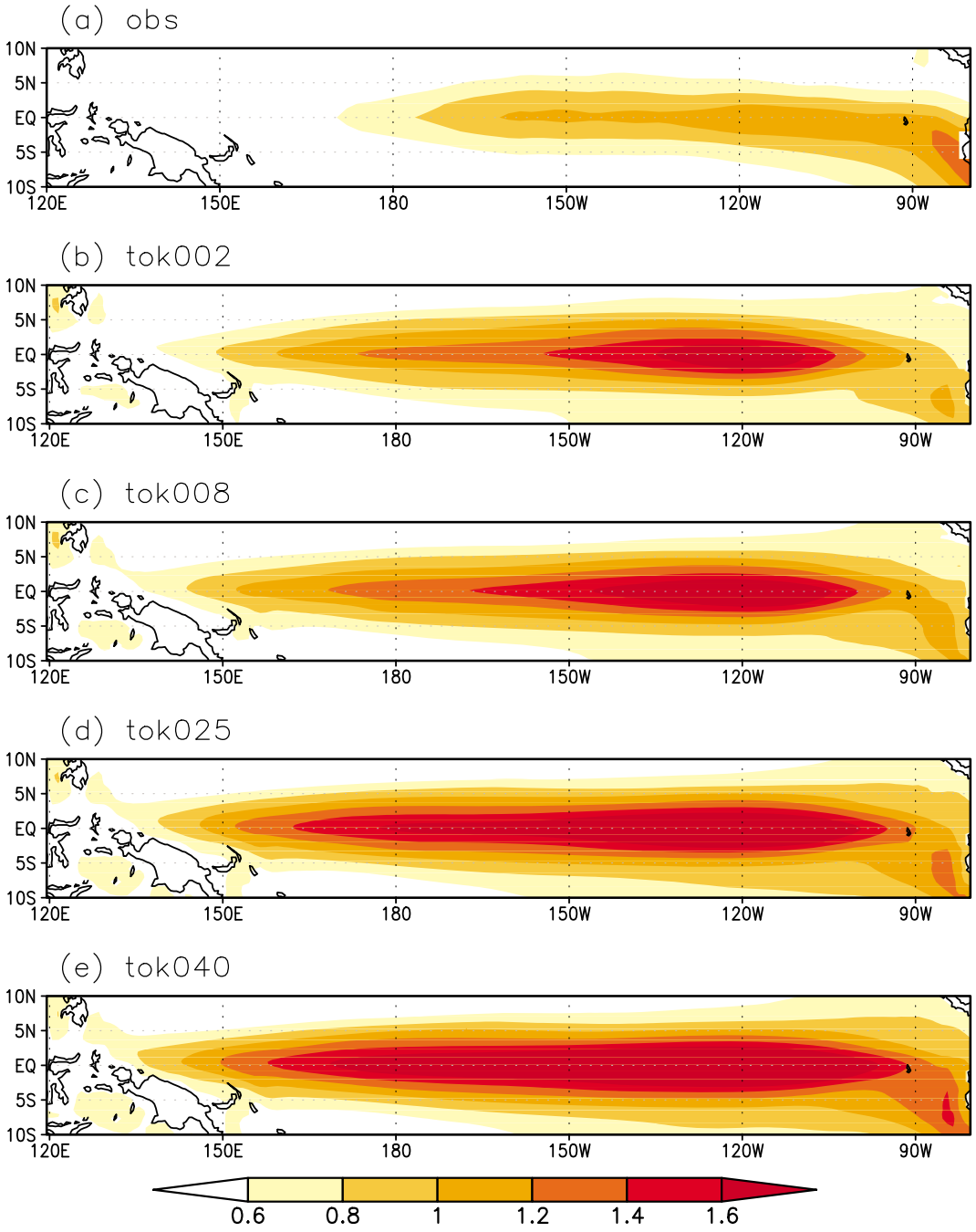

Figure 1. Standard deviation (°C) of monthly mean SST anomalies over the tropical Pacific in (a) observations, (b) tok002, (c) tok008, (d) tok025, and (e) tok040.

deviation of monthly mean SST anomalies from observations and all simulations. In all simulations, the maximum variability appears near 120°W, and the overall magnitude of variability increases with the Tokioka parameter. The amplitudes of ENSO simulated in the experiments are larger than that in the observations, as consistent with the results shown in the work of *Wittenberg et al.* [2006]. *Wittenberg et al.* [2006] showed that CM2.1 has the weaker atmospheric damping for the ENSO-related SST anomaly, which might contribute to the excessive ENSO in this model. The net surface heat flux anomaly associated with ENSO does not change much with the Tokioka parameter (see Figure 5a), so that the ENSO represented in our simulations has larger amplitude than that observed.

[11] Table 1 summarizes the sensitivity of the ENSO amplitude to the values of the Tokioka parameter. Changing the Tokioka parameter from 0.002 to 0.04 leads to about 30% increase of the standard deviation of Niño 3.4 SST anomaly (from 1.18 to 1.51°C). Furthermore, the increase of the standard deviation is monotonic from tok002 to tok040 to large extent. Interestingly, the relationship between the magnitude of the entrainment rate and the ENSO amplitude shown in Figure 1 and Table 1 seems to be opposite to that reported by *Watanabe et al.* [2011]. In our simulations using

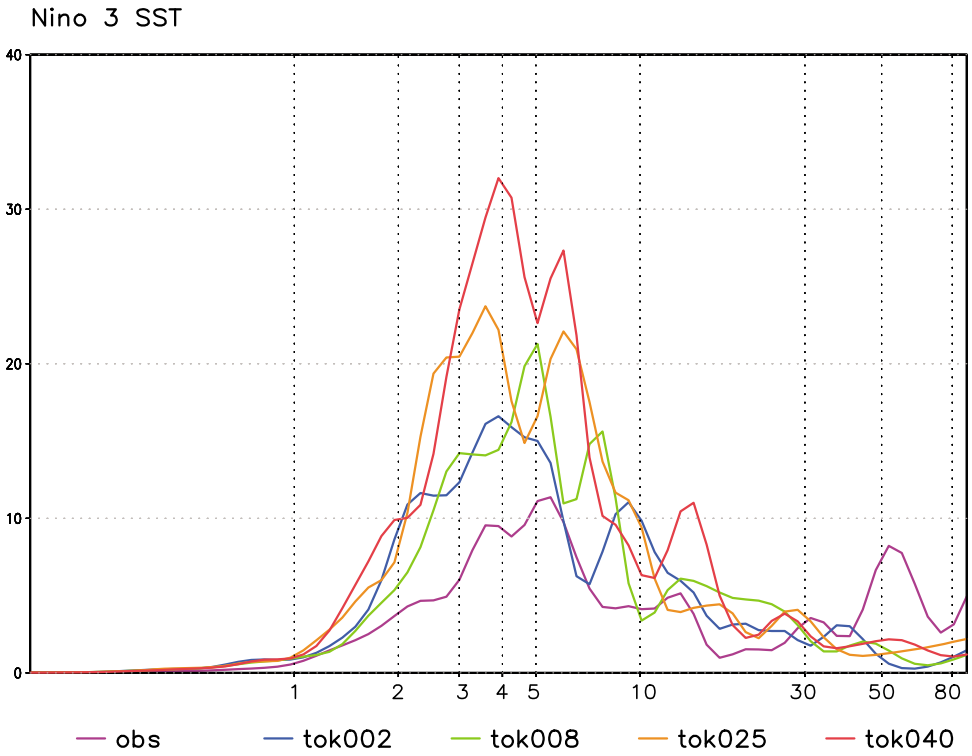

Figure 2. Power spectrum of Niño 3 indices in observations (purple line), tok002 (blue line), tok008 (green line), tok025 (orange line), and tok040 (red line).

CM2.1, the ENSO amplitude amplifies with a larger entrainment rate, while it contracts with a larger entrainment rate in MIROC5 simulations. The difference between two simulation sets will be further discussed in the latter part of this section.

[12] Figure 2 shows the power spectrum of Niño 3 indices from observations and the simulations. As observed, the dominant frequency of the interannual variability appears in the 2–7 year period in all simulations. Overall, the periodicity of ENSO seems similar in the four simulations. It is hard to find a systematic change with the Tokioka parameter, though there is some diversity in the shapes of the power spectrum among the simulations. It is conceived that the 200 year simulation is still too short to distinguish a slight change of ENSO periodicity unlike the ENSO amplitude. Furthermore, there is no notable difference between simulations in the meridional structure of the ENSO-related wind stress anomalies (Figure 3), which has been suggested as an indicator of the ENSO period in the CGCM simulations [*Kug et al.*, 2003; *Wittenberg et al.*, 2006; *Neale et al.*, 2008]. This suggests that the impacts of the Tokioka parameter are robust and systematic on the amplitude of ENSO, while there is no such a systematic variation in the frequency of ENSO.

[13] The ENSO mechanisms that have been suggested in the literature are investigated to find out the most relevant mechanism(s) behind the increase of the ENSO amplitude. In the work of *Wittenberg et al.* [2006] it is shown that the advection of warm (cold) water by the anomalous eastward (westward) equatorial current (i.e., zonal advective feedback) contribute to the development (decay) of ENSO simulated in the standard version of CM2.1 (tok025). Also shown is the recharge/discharge behavior of the equatorial upper ocean heat content associated with ENSO, which is induced by the zonal mean zonal wind stress variation [*Kug et al.*, 2010]. Our investigation suggests the atmospheric feedback processes as the mechanism responsible for the increase of the ENSO magnitude with the increase of the Tokioka parameter. In section 4 we discuss that other ENSO feedback processes are not suitable for explaining the changes in the ENSO magnitude we observed in this model.

[14] To compare the atmospheric responses to the ENSO-related SST anomalies, the monthly mean anomalies of precipitation and zonal wind stress are regressed against Niño 3 index (Figure 3). Positive precipitation anomalies appear over the Pacific in all simulations as responses to the anomalous SST anomalies related with ENSO. Accompanied by the positive precipitation anomaly is the anomalous westerly, which commonly extends to about 140°E in the simulations. When there is a preexisting SST anomaly in the central/eastern Pacific, the anomalous westerly further enhances the SST anomaly via zonal advective feedback and thermocline feedback [*Li*, 1997; *An and Jin*, 2001]. Although gross feature is similar to each other, it is evident in Figure 3 that the anomalous precipitation and westerly winds gradually shift toward the east with the larger Tokioka parameter values. For example, the maximum precipitation is near 160°E in the experiments with the small Tokioka parameter values (i.e., tok002 and tok008), while it is near the dateline (i.e., 180°E) for tok040. According to the shift in the position of the precipitation anomalies, the zonal wind stress anomaly also shifts to the east as Tokioka parameter value becomes larger.

[15] We mentioned at the end of the first paragraph in section 3 that our results looked opposite to those by

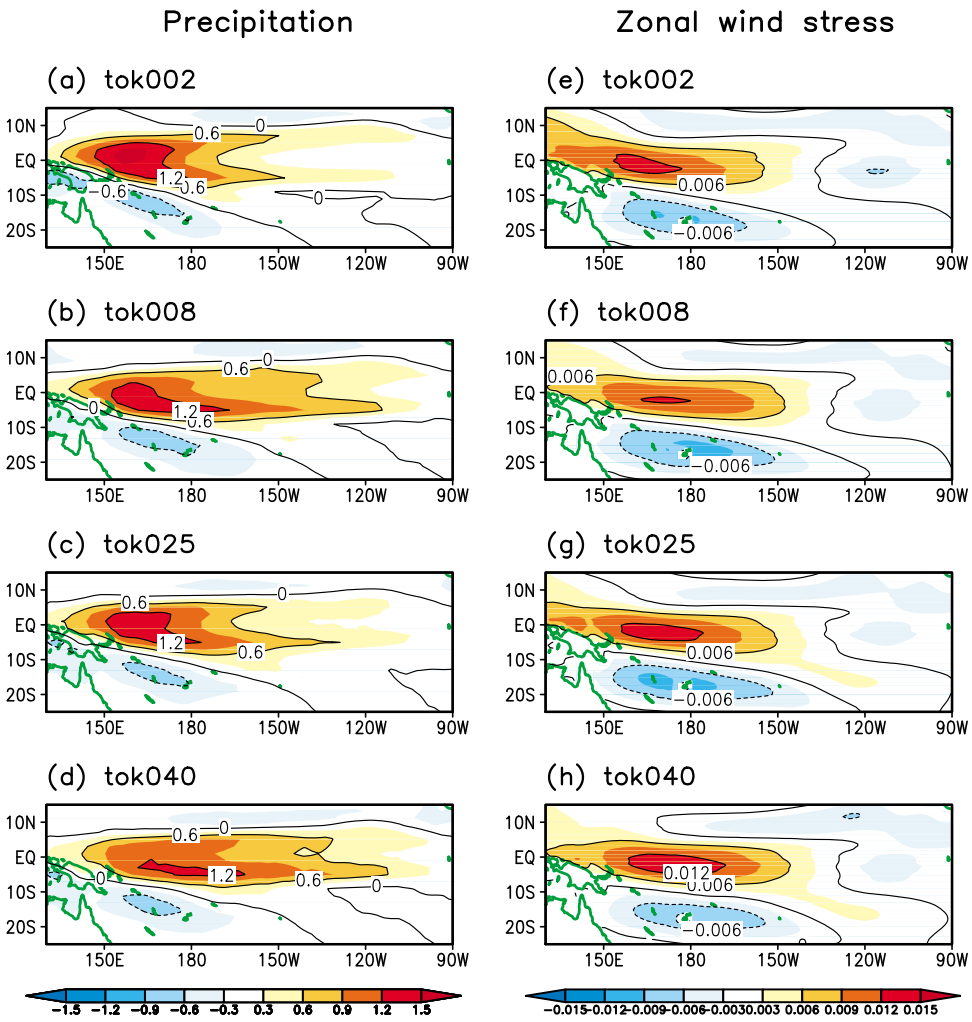

Figure 3. Monthly mean anomalies of precipitation (mm d^{-1} K^{-1}) and zonal wind stress (N m^{-2} K^{-1}) regressed on the Niño 3.4 SST time series in (a and e) tok002, (b and f) tok008, (c and g) tok025, and (d and h) tok040.

Watanabe et al. [2011] in terms of the relationship between the entrainment rate and the ENSO magnitude. The ENSO amplitude simulated in two different models, however, are commonly linked to the geographical location of the ENSO-related atmospheric anomalies in a consistent manner. In both studies, the ENSO magnitude is larger in the experiment with the ENSO-related atmospheric anomalies located further to the east. The results from the two models suggest that the amplitude of the ENSO variability simulated in a CGCM is closely related to the position of the ENSO-related precipitation/wind stress anomalies. *Wittenberg et al.* [2006] showed that this relationship also held between CM2.1 with CM2.0; CM2.1 simulated the larger amplitude of ENSO and the eastward shifted ENSO-related zonal wind stress anomaly compared to those in CM2.0.

[16] The position of the atmospheric response to the ENSO-related SST anomaly can be quite critical in determining the ENSO amplitude. If the wind stress anomalies are shifted to the east and become more close to the eastern Pacific, wind stress forcing more effectively deepens the thermocline over the eastern Pacific. This stronger atmospheric feedback process implies a larger SST variability over the eastern Pacific. *Kang and Kug* [2002] tested this hypothesis by varying the zonal location of the ENSO-related zonal wind stress anomalies in an intermediate-complexity coupled model. They demonstrated that the ENSO amplitude increased 10 times when the location of the anomalous wind stress was changed from 170°E to 170°W [*Kang and Kug*, 2002, Figure 6]. The increase of the ENSO amplitude was attributed to the enhanced thermocline response in the eastern Pacific. *Watanabe et al.* [2011] also showed that the subsurface temperature anomalies over the eastern Pacific were much stronger when the zonal location of wind stress was shifted to the east.

[17] The position of the ENSO-related wind stress/precipitation anomalies might be related with the mean climate state over the tropical Pacific, which is altered with the Tokioka parameter in this model. Therefore, it is worthwhile examining how the mean state changes with the Tokioka parameter although a full understanding of the changes in the tropical Pacific mean state with varying Tokioka parameter is beyond the scope of the current study. Here we propose a plausible hypothesis regarding the mean state change on the basis of the background knowledge about

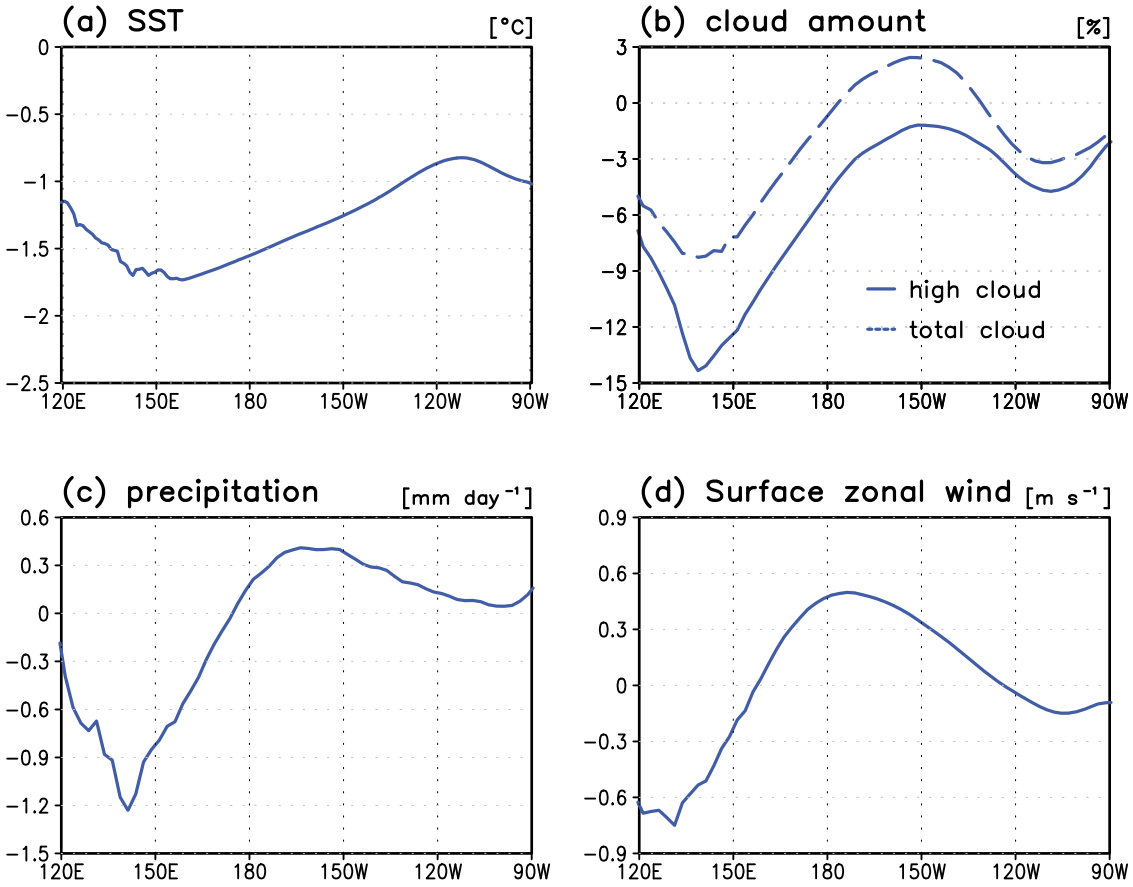

Figure 4. (a) Zonal structure for the difference of the annual mean climatological SST (°C) between tok002 and tok040 (tok040 minus tok002). (b) As in Figure 4a but for high cloud amount (solid line, percent) and total cloud amount (dashed line, percent). (c) As in Figure 4a but for precipitation (mm d^{-1}). (d) As in Figure 4a but for zonal wind (m s^{-1}) in surface. All variables are averaged between 10°S and 10°N.

the convection scheme, and role of high clouds on Earth's climate.

[18] Because the mean state response is almost linear to values of the Tokioka parameter, we only show the difference between two extreme cases (tok040 minus tok002) in order to show the mean state changes. Figure 4a shows the mean SST difference over the tropical Pacific. It is clear that a basin-wide cooling occurs in the simulation with the larger Tokioka parameter. This basin-wide cooling is accompanied by the reduction of high clouds (Figure 4b), which implies that, in a same atmospheric condition, more longwave radiation escapes with the large Tokioka parameter. Because the high cloud is maintained by deep convection to large extent, it might be reduced when deep convection is suppressed with the larger Tokioka parameter value. The SST decrease due to the reduction of the high cloud leads to precipitation decrease with reduction of total cloud as well as high clouds. As a result, when the Tokioka parameter is increased, the amount of cloud in the atmosphere, precipitation, and SST decreases in the tropical Pacific, especially in the western Pacific (Figure 4). This means the east–west asymmetry in the tropical Pacific becomes smaller when the larger Tokioka parameter value is used. It is not understood why the mean state changes are relatively larger in the western part of the tropical Pacific, compared to that in the eastern part. Perhaps, the change of Tokioka parameter will be more effective where the deep convection is dominant. Therefore, the mean state over the western Pacific will be more sensitive than that over the eastern Pacific, where the deep convection is highly suppressed.

[19] The reduction of the east–west asymmetry in the tropical Pacific, which is resulted from adjustment processes of the ocean-atmosphere coupled system to the changes of the Tokioka parameter, accompanies the increase of mean rainfall over the eastern Part of the basin (Figure 4c). Figure 5a shows that the mean precipitation over the Niño 3 region monotonically increases with the weakening of the zonal SST gradient, defined here as a difference between the mean SST values over the Niño 4 and Niño 3 regions. This suggests that the eastern Pacific mean precipitation is closely related to the east–west SST asymmetry in the tropical Pacific. For similar SST asymmetry, model simulates mean precipitation over the Niño 3 region larger than that observed, possibly due to model bias.

[20] It is widely accepted that a distribution of underlying SST plays a major role in determining a distribution of precipitation, so that rain mostly occurs over the area where SST exceeds a threshold value. The threshold SST might change in different climate, such as those in our simulations with varying Tokioka parameter. In this sense, the increase

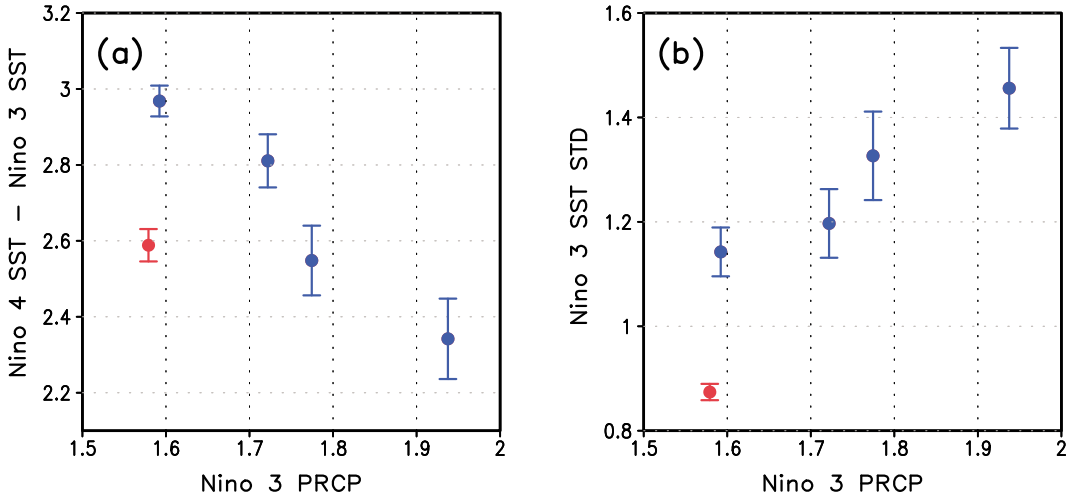

Figure 5. Scatterplot of (a) the mean SST gradient (between Niño 4 and Niño 3 regions) against the mean Niño 3 precipitation and (b) the standard deviation of Niño 3 SST against the mean Niño 3 precipitation from observations (red) and the simulations (blue). The scale bar represents a range of internal variability, which is calculated by one standard deviation of 50 year sampling in a bootstrap method.

in precipitation over the Niño 3 region with the larger Tokioka parameter might be understood as a result of the reduction of the threshold SST value. The basin wide cooling would reduce the threshold SST. In addition to this, the fact that more reduction occurred in the relatively higher-SST region also suggests a reduction of the SST threshold.

[21] Furthermore, the mean precipitation over the Niño 3 region has an approximately linear relationship with the ENSO amplitude (Figure 5b). Compared to the model simulations, observations exhibit relatively smaller amount of mean precipitation over the Niño 3 region as well as weaker ENSO amplitude. *Ham and Kug* [2011] also showed in a multimodel framework that the eastern Pacific dryness is closely related to the extent of SST development in the eastern Pacific. That is, the eastern Pacific SST anomalies are highly suppressed when the eastern Pacific mean precipitation is too dry. Here we argue that the climatological precipitation over the central to eastern Pacific is related with the interannual variability of precipitation there. As mentioned above, increase of the climatological precipitation over the Niño 3 region might be due to the reduction of SST threshold. With the lower SST threshold, a same SST anomaly associated with ENSO might induce anomalous precipitation more easily than with a higher SST threshold. This could be interpreted as follows; if the mean climate over the eastern Pacific is relatively dry, it would be relatively more difficult to have a large interannual variation of precipitation in that region. This is because positive SST anomalies would hardly produce precipitation anomalies if there is a strong underlying climatological sinking motion. Therefore, when the climatological convection is more suppressed in the eastern Pacific, the anomalous precipitation and wind stress associated with the eastern Pacific SST forcing would be more confined to the western-central Pacific. As mentioned above the effectiveness of a wind stress anomaly to deepen the thermocline over the eastern Pacific becomes weaker as it moves toward west. In our simulation set, the larger Tokioka parameter leads to the increasing mean precipitation over the eastern Pacific, which induces the eastward shift of the atmospheric feedback associated with the eastern Pacific warming, which then results in the stronger ENSO variability.

4. Discussion

4.1. CM2.1 Versus MIROC5

[22] It is worthwhile to compare our results with those in the work of *Watanabe et al.* [2011]. In their results, the ENSO amplitude increases with the decreasing entrainment rate. In our results, the amplitude of ENSO increases with a larger Tokioka parameter value, which corresponds to an enhanced entrainment rate diagnosed in the convection scheme [*Moorthi and Suarez*, 1992]. This is because the larger Tokioka parameter value inhibits convective plumes with small entrainment rates (see section 2). Therefore, it seems that the relationships between the entrainment rate in the convection scheme and the ENSO amplitude are opposite in the two studies. What is consistent is that the east–west asymmetry of the SST in the Pacific basin is relatively small in the simulations with a relatively larger ENSO amplitude.

[23] Although the mean SST decreases in both models when the entrainment rate is increased, the zonal distributions of the SST change are different from each other. A relatively stronger cooling occurs over the western (eastern) Pacific in CM2.1 (MIROC5). As a result, in one model (MIROC5), the east–west asymmetry of the mean SST becomes larger with a large entrainment rate, while it decreases in another model (CM2.1). In MIROC5, the changes in the high-cloud amount are found in the entire tropical Pacific (M. Watanabe, personal communication, 2011), while it is large in the western Pacific in CM2.1. This suggests that the changes in longwave fluxes through the perturbed amount of high clouds play an active role in determining the Pacific basin SST distribution, though it is currently uncertain why the two models exhibit different responses. The ENSO simulated in the two sets of

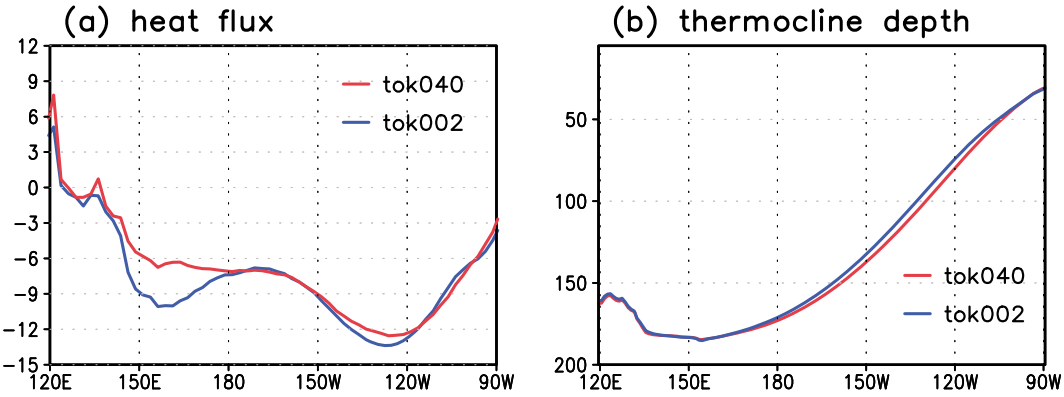

Figure 6. (a) Zonal structure of the monthly mean anomalies of total heat flux regressed on the Niño 3 SST time series in tok040 (red line) and tok002 (blue line). (b) Annual mean climatological thermocline in tok040 and tok002. The variables are averaged between 10°S and 10°N.

simulations using two different models demonstrate that modifications in the cumulus parameterization of the GCM can affect ENSO amplitude through changes in the mean state.

4.2. Other ENSO Feedbacks

[24] In this study, we mainly focused on a specific aspect of the ENSO mechanisms, which is atmospheric feedback through wind stress over the Pacific. This is because other ENSO mechanisms play minor role in determining sensitivity of ENSO magnitude to the Tokioka parameter in the present simulations. Here we will briefly discuss changes in the other feedback processes related to ENSO magnitude. The heat flux anomalies regressed against the Niño 3 index over the central-eastern Pacific region are similar to each other (Figure 6a), indicating the atmospheric damping is a minor player in determining ENSO amplitude changes in the present sensitivity experiments. Regarding the thermocline feedback, the structure of thermocline depth also does not change dramatically (Figure 6b), which is consistent with surface wind changes. In addition, regarding the zonal advective feedback mechanism [*An and Jin*, 2001; *Picaut et al.*, 1997], we showed in Figure 4a that zonal gradient of SST was reduced with larger Tokioka parameter. The weakened zonal gradient of SST leads to weaker zonal advective feedback, preferring weak ENSO variability, which is inconsistent with our results shown in Figure 1. These results indicate that the changes in ocean basic state play a minor role in determining ENSO amplitude in our sensitivity experiments.

[25] We attributed the changes in mean rainfall pattern mostly to the reduced east–west SST gradient, indicating that it is result of air-sea coupled process. However, one may argue that the increase in Tokioka parameter is directly responsible for the changes in rainfall pattern. We found that results from previous works do not support this hypothesis. *Sobel et al.* [2010, Figure 11] and *Kim et al.* [2011, Figures 4 and 5] presented mean rainfall pattern simulated using AM2 AGCM experiments with different Tokioka parameters. Their results show a westward shift in the mean rainfall with larger Tokioka parameter, which is the opposite to the present results in coupled model. Therefore, it is conceived that the eastern Pacific wetness can be mostly attributed to the changes in SST, which is a result of air-sea coupled processes.

5. Summary and Conclusion

[26] A series of 200 year long simulations was conducted using GFDL CM2.1, by varying the Tokioka parameter in the cumulus parameterization of the model. The Tokioka modification [*Tokioka et al.*, 1988] suppresses a convective plume when the entrainment rate of the plume is less than a threshold that varies inversely with the PBL depth. In the modification, a constant, called the Tokioka parameter, determines the triggering strength and mean value of the entrainment rate. It is found from the simulations that the magnitude of ENSO simulated in this model amplifies as the Tokioka parameter increases. Changing the Tokioka parameter from 0.002 to 0.04 results in an increase of the standard deviation of the Niño 3.4 SST anomaly (from 1.18 to 1.51°C) by about 30%.

[27] The location of the anomalous precipitation and westerly wind stress related to the ENSO gradually shifts toward the east in the experiments as the Tokioka parameter increases. If the wind stress anomalies are shifted to the east in the equatorial region, the effects of the wind stress anomalies on the thermocline of the eastern Pacific become larger so that the ENSO variability can be enhanced [*Kang and Kug*, 2002]. The eastward shift of the ENSO-related atmospheric anomalies is resulted from the changes in the mean state over the Pacific basin. The high cloud is reduced when deep convection is suppressed as the Tokioka parameter increases. The fractional change is relatively larger in the western Pacific, and as a result, the east–west asymmetries in the Pacific basin mean SST, precipitation, and high clouds are reduced with a larger Tokioka parameter value. The results in this study are compared to those of *Watanabe et al.* [2011]. The ENSO simulated in the two sets of experiments demonstrate that the change in the cumulus parameterization can affect the ENSO amplitude differently because changes in the mean state are different in different models. In one model (MIROC5), the east–west SST asymmetry becomes larger with a large entrainment rate, while it becomes smaller in another model (CM2.1). In both studies, however, the simulated ENSO amplitude can be explained by the east–west asymmetry in the Pacific basin mean SST distri-

bution. Our study suggests that the east–west asymmetry in the Pacific basic mean state is an important metrics for climate model, while the link between parameterizations of atmospheric model and the asymmetry need be further understood.

[28] A challenge of simulating a reasonable magnitude of ENSO variability with CGCMs is related to another challenge of reducing uncertainty in climate change projection using the same models. The sensitive ENSO characteristics simulated in CGCMs to one parameter in the model, calls for two future works to overcome the challenge of the reliable climate change projection. One is to find other parameters that have significant impacts on the ENSO variability simulated. The perturbed physics ensemble [*Sanderson et al.*, 2008] would be an ideal framework for this purpose. The other is to provide additional constraint on the parameters, such as entrainment rate, using observations [*Luo et al.*, 2010] and cloud-permitting high-resolution simulations.

[29] **Acknowledgments.** This work is supported by a National Research Foundation of Korea grant funded by the Korean Government (MEST; NRF-2009-C1AAA001-2009-0093042). D.K. was supported by NASA grant NNX09AK34G.

References

An, S.-I., and F.-F. Jin (2001), Collective role of thermocline and zonal advective feedbacks in the ENSO mode, *J. Clim.*, *14*, 3421–3432, doi:10.1175/1520-0442(2001)014<3421:CROTAZ>2.0.CO;2.

Delworth, T. L., et al. (2006), GFDL's CM2 global coupled climate models. part I: Formulation and simulation characteristics, *J. Clim.*, *19*, 643–674, doi:10.1175/JCLI3629.1.

Frierson, D. M. W., D. Kim, I.-S. Kang, M. Lee, and J.-I. Lin (2011), Structure of AGCM simulated convectively coupled equatorial waves and sensitivity to convective parameterization, *J. Atmos. Sci.*, *68*, 26–45, doi:10.1175/2010JAS3356.1.

Gnanadesikan, A., et al. (2006), GFDL's CM2 global coupled climate models. Part II: The baseline ocean simulation, *J. Clim.*, *19*, 675–697, doi:10.1175/JCLI3630.1.

Griffies, S. M., et al. (2005), Formulation of an ocean model for global climate simulations, *Ocean Sci.*, *1*, 45–79, doi:10.5194/os-1-45-2005.

Guilyardi, E., et al. (2009a), Understanding El Niño in ocean-atmosphere general circulation models: Progress and challenges, *Bull. Am. Meteorol. Soc.*, *90*, 325–340, doi:10.1175/2008BAMS2387.1.

Guilyardi, E., P. Braconnot, F.-F. Jin, S. T. Kim, M. Kolasinski, T. Li, and I. Musat (2009b), Atmosphere feedbacks during ENSO in a coupled GCM with a modified atmospheric convection scheme, *J. Clim.*, *22*, 5698–5718, doi:10.1175/2009JCLI2815.1.

Ham, Y.-G., and J.-S. Kug (2011) How well do current climate models simulate two-types of El Niño?, *Clim. Dyn.*, doi:10.1007/s00382-011-1157-3, in press.

Ham, Y.-G., J.-S. Kug, I.-S. Kang, F.-F. Jin, and A. Timmermann (2010), Impact of diurnal atmosphere-ocean coupling on tropical climate simulations using a coupled GCM, *Clim. Dyn.*, *34*, 905–917, doi:10.1007/s00382-009-0586-8.

Held, I. M., and M. Zhao (2008), horizontally homogeneous rotating radiative–convective equilibria at GCM resolution, *J. Atmos. Sci.*, *65*, 2003–2013, doi:10.1175/2007JAS2604.1.

Kang, I.-S., and J.-S. Kug (2002), El Niño and La Niña sea surface temperature anomalies: Asymmetry characteristics associated with their wind stress anomalies, *J. Geophys. Res.*, *107*(D19), 4372, doi:10.1029/2001JD000393.

Kang, S. M., I. M. Held, D. M. W. Frierson, and M. Zhao (2008), The response of the ITCZ to extratropical thermal forcing: Idealized slab-ocean experiments with a GCM, *J. Clim.*, *21*, 3521–3532, doi:10.1175/2007JCLI2146.1.

Kim, D., J.-S. Kug, I.-S. Kang, F.-F. Jin, and A. Wittenberg (2008), Tropical Pacific impacts of convective momentum transport in the SNU coupled GCM, *Clim. Dyn.*, *31*, 213–226, doi:10.1007/s00382-007-0348-4.

Kim, D., A. H. Sobel, D. M. W. Frierson, E. D. Maloney, and I.-S. Kang (2011), A systematic relationship between intraseasonal variability and mean state bias in AGCM simulations, *J. Clim.*, doi:10.1175/2011JCLI4177.1, in press.

Knutson, T. R., T. L. Delworth, K. W. Dixon, I. M. Held, J. Lu, V. Ramaswamy, M. D. Schwarzkopf, G. Stenshikov, and R. J. Stouffer (2006), Assessment of twentieth-century regional surface temperature trends using the GFDL CM2 coupled models, *J. Clim.*, *19*, 1624–1651, doi:10.1175/JCLI3709.1.

Kug, J.-S., I.-S. Kang, and S.-I. An (2003), Symmetric and antisymmetric mass exchanges between the equatorial and off-equatorial Pacific associated with ENSO, *J. Geophys. Res.*, *108*(C8), 3284, doi:10.1029/2002JC001671.

Kug, J.-S., J. Choi, S.-I. An, F.-F. Jin, and A. T. Wittenberg (2010), Warm pool and cold tongue El Niño events as simulated by the GFDL 2.1 coupled GCM, *J. Clim.*, *23*, 1226–1239, doi:10.1175/2009JCLI3293.1.

Lee, M.-I., S. D. Schubert, M. J. Suarez, J.-K. E. Schemm, H.-L. Pan, J. Han, and S.-H. Yoo (2008), Role of convection triggers in the simulation of the diurnal cycle of precipitation over the United States Great Plains in a general circulation model, *J. Geophys. Res.*, *113*, D02111, doi:10.1029/2007JD008984.

Li, T. (1997), Phase transition of the El Niño–Southern Oscillation: A stationary SST mode, *J. Atmos. Sci.*, *54*, 2872–2887, doi:10.1175/1520-0469(1997)054<2872:PTOTEN>2.0.CO;2.

Li, T., and T. F. Hogan (1999), The role of the annual mean climate on seasonal and interannual variability of the tropical Pacific in a coupled GCM, *J. Clim.*, *12*, 780–792, doi:10.1175/1520-0442(1999)012<0780:TROTAM>2.0.CO;2.

Luo, Z. J., G. Y. Liu, and G. L. Stephens (2010), Use of A Train data to estimate convective buoyancy and entrainment rate, *Geophys. Res. Lett.*, *37*, L09804, doi:10.1029/2010GL042904.

Moorthi, S., and M. J. Suarez (1992), Relaxed Arakawa-Schubert; A parameterization of moist convection for general circulation models, *Mon. Weather Rev.*, *120*, 978–1002, doi:10.1175/1520-0493(1992)120<0978:RASAPO>2.0.CO;2.

Neale, R. B., J. H. Richter, and M. Jochum (2008), The impact of convection on ENSO: From a delayed oscillator to a series of events, *J. Clim.*, *21*, 5904–5924, doi:10.1175/2008JCLI2244.1.

Picaut, J., F. Masia, and Y. du Penhoat (1997), An advective reflective conceptual model for the oscillatory nature of the ENSO, *Science*, *277*, 663–666, doi:10.1126/science.277.5326.663.

Sanderson, B. M., et al. (2008), Constraints on model response to greenhouse gas forcing and the role of subgrid-scale processes, *J. Clim.*, *21*, 2384–2400, doi:10.1175/2008JCLI1869.1.

Sobel, A. H., E. D. Maloney, G. Bellon, and D. M. Frierson (2010), Surface fluxes and tropical intraseasonal variability: A reassessment, *J. Adv. Model. Earth Syst.*, *2*(2), 1–27, doi:10.3894/JAMES.2010.2.2.

Stevenson, S., B. Fox-Kemper, M. Jochum, B. Rajagopalan, and S. G. Yeager (2010), ENSO Model Validation Using Wavelet Probability Analysis, *J. Clim.*, *23*, 5540–5547, doi:10.1175/2010JCLI3609.1.

Tokioka, T., K. Yamazaki, A. Kitoh, and T. Ose (1988), The equatorial 30–60 day oscillation and the Arakawa-Schubert penetrative cumulus parameterization, *J. Meteorol. Soc. Jpn.*, *66*, 883–901.

Watanabe, M., M. Chikira, Y. Imada, and M. Kimoto (2011), Convective control of ENSO simulated in MIROC, *J. Clim.*, *24*, 543–562, doi:10.1175/2010JCLI3878.1.

Wittenberg, A. T., A. Rosati, N.-C. Lau, and J. J. Ploshay (2006), GFDL's CM2 global coupled climate models. Part III: Tropical Pacific climate and ENSO, *J. Clim.*, *19*, 698–722, doi:10.1175/JCLI3631.1.

Wittenberg, A. T. (2009), Are historical records sufficient to constrain ENSO simulations?, *Geophys. Res. Lett.*, *36*, L12702, doi:10.1029/2009GL038710.

Wu, X., L. Deng, X. Song, G. Vettoretti, W. R. Peltier, and G. J. Zhang (2007), Impact of a modified convective scheme on the Madden-Julian Oscillation and El Niño-Southern Oscillation in a coupled climate model, *Geophys. Res. Lett.*, *34*, L16823, doi:10.1029/2007GL030637.

Y.-S. Jang, Y.-H. Kim, and J.-S. Kug, Korea Ocean Research and Development Institute, Ansan 426-744, South Korea. (jskug@kordi.re.kr)

F.-F. Jin, Department of Meteorology, University of Hawai'i at Mānoa, 2525 Correa Rd., Bldg. HIG 350, Honolulu, HI 96822, USA.

D. Kim, Lamont-Doherty Earth Observatory, Columbia University, 61 Rt. 9w, Palisades, NY 10964, USA.

D.-H. Kim, Department of Atmospheric Science, Yonsei University, 134 Shinchon-dong, Seodaemun-gu, Seoul 120-749, South Korea. (dohnkim@gmail.com)

M. Watanabe, Atmosphere and Ocean Research Institute, University of Tokyo, 5-1-5 Kashiwanoha, Kashiwa, Chiba 277-8568, Japan.